

GENOMICS.  
TRANSCRIPTOMICS

UDC 577.2+577.29

## APP<sup>swe</sup>/PS1<sup>dE9</sup>/Blg Transgenic Mouse Line for Modeling Cerebral Amyloid Angiopathy Associated with Alzheimer's Disease

E. A. Lysikova<sup>a, \*</sup>, E. V. Kuzubova<sup>b</sup>, A. I. Radchenko<sup>b</sup>, E. A. Patrakhanov<sup>b</sup>, K. D. Chaprov<sup>a, b</sup>,  
M. V. Korokin<sup>b</sup>, A. V. Deykin<sup>b</sup>, O. S. Gudyrev<sup>b</sup>, and M. V. Pokrovskii<sup>b</sup>

<sup>a</sup> *Institute of Physiologically Active Compounds, Russian Academy of Sciences, Chernogolovka, 142432 Russia*

<sup>b</sup> *Belgorod State University, Belgorod, 308015 Russia*

\**e-mail: lysikova.ipac@gmail.com*

Received June 8, 2022; revised July 30, 2022; accepted July 30, 2022

**Abstract**—Alzheimer's disease (AD) is the most common proteinopathy, which is accompanied by a steady decrease in the patient's cognitive functions with a simultaneous accumulation of amyloid plaques in brain tissues. Amyloid plaques are extracellular aggregates of amyloid  $\beta$  (A $\beta$ ) and are associated with neuroinflammation and neurodegeneration. Unlike humans and all other mammals, rats and mice do not reproduce AD-like pathology because there are three amino acid substitutions in their A $\beta$ . Amyloid plaques form in the brains of transgenic mice with overexpression of human A $\beta$ , and such mice are therefore possible to use in biomedicine to model the key features of AD. The transgenic mouse line APP<sup>swe</sup>/PS1<sup>dE9</sup> is widely used as an animal model to study the molecular mechanisms of AD. A study was made to characterize the APP<sup>swe</sup>/PS1<sup>dE9</sup>/Blg subline, which was obtained by crossing APP<sup>swe</sup>/PS1<sup>dE9</sup> mice on a CH3 genetic background with C57Bl6/Chg mice. No difference in offspring's survival and fertility was observed in the subline compared to wild-type control mice. Histological analysis of the brain in the APP<sup>swe</sup>/PS1<sup>dE9</sup>/Blg line confirmed the main neuromorphological features of AD and showed that amyloid plaques progressively increase in number and size during aging. The APP<sup>swe</sup>/PS1<sup>dE9</sup>/Blg line was assumed to provide a convenient model for developing therapeutic strategies to slow down AD progression.

**Keywords:** Alzheimer's disease, transgenic mice, amyloid  $\beta$ , cerebral amyloid angiopathy

**DOI:** 10.1134/S0026893323010077

### INTRODUCTION

Alzheimer's disease (AD) is a neurodegenerative disorder and the most common form of dementia [1]. AD is classed with proteinopathies, in which an important pathogenetic role is played by structural changes or metabolic alterations in aggregation-prone proteins. AD is characterized by a slow progression of the pathological process and has a long prodromal stage [2]. There is still no effective means to treat AD, and a high prevalence makes AD an important social problem.

In the early 20th century, the German psychiatrist Alois Alzheimer detected inclusions (senile plaques) in pathohistological preparations of brain tissues of demented patients. An aggregated amyloid  $\beta$  (A $\beta$ ) peptide was identified more recently as a major component of senile plaques. The A $\beta$  peptide is a hydrolysis product of the amyloid precursor protein (APP) [3]. An amyloid cascade hypothesis, which is commonly accepted now, suggests that cerebral amyloidosis

triggers other pathological processes in AD progression [4].

APP is a type 1 transmembrane protein expressed in many tissues and has three main isoforms: APP695, APP751, and APP770. The APP695 is major in neurons, while APP751 and APP770 are predominantly expressed in other cells [5]. APP plays an important role in neurite growth and axon branching in the developing brain and is involved in synaptogenesis and synaptic plasticity maintenance [5]. APP is normally processed via a nonamyloidogenic pathway and is consecutively cleaved within the A $\beta$  domain by  $\alpha$ - and  $\gamma$ -secretases to produce nonpathogenic fragments, sAPP $\alpha$  and C-terminal fragments (CTFs) [6]. The soluble form sAPP $\alpha$  possesses neurotrophic activity and is involved in protecting neurons against excitotoxicity by regulating calcium homeostasis [5]. Consecutive proteolytic cleavage of APP by  $\beta$ - and  $\gamma$ -secretases yields the A $\beta$  peptide, which is capable of aggregation, and nonpathogenic fragments [7]. The two most common forms of the A $\beta$  peptide consist of 40 (A $\beta$ 40) and 42 (A $\beta$ 42) amino acid residues, and the A $\beta$ 42 form is more toxic to the cell [8].

*Abbreviations:* AD, Alzheimer's disease; APP, amyloid precursor protein; PSEN1, presenilin 1.

AD is thought to be a multifactorial disorder; its sporadic forms with later onset (at more than 65 years of age) are the most common. Studies of familial AD forms with younger onset (before the age of 65) have revealed the genetic factors that are associated with early development of neurodegenerative processes in the patient's brain. Several mutations of the *APP* gene are now known to substantially increase the A $\beta$ 42 level and are associated with early-onset AD [9]. Mutations have additionally been described in the presenilin 1 (*PSEN1*) and presenilin 2 (*PSEN2*) genes, which code for transmembrane proteins of the endoplasmic reticulum. Genomic studies have revealed more than 170 *PSEN1* and 13 *PSEN2* mutations associated with the most common forms of familial early-onset AD [7]. The *PSEN1* and *PSEN2* proteins are components of the  $\gamma$ -secretase complex and affect the APP processing [10]. *PSEN1* mutations increase the specificity of APP cleavage to the toxic A $\beta$ 42 peptide by  $\gamma$ -secretase [11], which is confirmed by the fact that the plasma A $\beta$ 42/A $\beta$ 40 ratio in patients carrying mutant *PSEN1* is higher than in patients with sporadic AD [12].

Animal models have been designed to study the molecular mechanisms that underlie the AD origin and progression. Transgenic mouse lines that reproduce progressive cerebral amyloidosis characteristic of AD are among the most adequate and common models. Transgenic cassettes with the most common mutations of genes associated with hereditary AD forms have been inserted in the mouse genome. First-generation models are mostly based on overexpression of cDNAs of the mutant human *APP* or *PSEN1* and reproduce the main pathological features of AD. Second-generation mouse models are knock-in models, in which regions carrying the Swedish (NL), Iberian (F), or Arctic (G) mutations have been used to replace the respective regions of the mouse *App* gene (*App*<sup>NL-G-F</sup>). A third-generation transgenic mouse line carries knock-in mutations of both *App* and *Psen1* (*App*<sup>NL-F</sup> *Psen1*<sup>P117L/WT</sup>) [13]. Table 1 summarizes the data on the transgenic animals that reproduce the formation of amyloid inclusions, which is the main pathological process in AD.

The pathological phenotype varies in each line, depending on the genetic background, rearing conditions, and the duration of isolated colony maintenance at the same breeding facility. The APP<sup>swe</sup>/PS1<sup>dE9</sup> subline was characterized in detail in our study.

The genome of APP<sup>swe</sup>/PS1<sup>dE9</sup> transgenic mice contains two transgenic cassettes integrated in the same locus of chromosome 9. One transgenic cassette contains cDNA of chimeric, A $\beta$  domain-humanized, *APP* with the Swedish mutation (K670N/M671L) under the control of the mouse prion protein gene promoter. The other transgenic cassette contains cDNA of human *PSEN1* with a deletion of exon 9 (PS1 $\Delta$ E9) under the control of the mouse prion protein gene promoter. Borchelt and colleagues [19] have con-

structed the double-transgenic APP/PS1 line by coinjecting linearized and purified plasmid DNAs into the pronucleus of a mouse zygote. Simultaneous incorporation of both of the transgenes was observed in 10% of mice after coinjection of the transgenic cassettes [31]. A line with the greatest transgenic cassette copy number was selected and used in further experiments. High levels of transgenic *PSEN1* and transgenic *APP* in the brains of model mice were confirmed by immunoblotting [19].

To construct transgenic animals, a fragment of the mouse prion protein gene (*PrP*) was modified in the Bluescript KS+ vector. The *PrP* fragment, which was designated phgPrP, contained an approximately 6-kb sequence upstream of the transcription start site, coding exon 1, intron 1, the mouse *PrP* coding region fused with exon 2, and approximately 3 kb of the 3'-untranslated region. The open reading frame of the phgPrP fragment was replaced with a XhoI restriction site. The resulting modified vector was designated MoPrP.Xho. A full-size human *PSEN1* dDNA, which coded for a protein with a deletion of amino acid residues 290–319 and was flanked with XhoI sites, was inserted into the XhoI site between exons 2 and 3 of mouse *PrP* in the MoPrP.Xho vector. A cDNA coding for the amyloid precursor protein with the humanized A $\beta$  domain and the Sweden mutation (K670N/M671L) was also cloned in the MoPrP.Xho vector between *PrP* exons 2 and 3 [19]. Each transgene was expressed under the control of the mouse *PrP* promoter. The promoter is active during embryo development and, in adults, ensures transgene expression predominantly in astrocytes and neurons of the central nervous system [31].

## EXPERIMENTAL

**Laboratory animals.** We used the APP<sup>swe</sup>/PS1<sup>dE9</sup>/Blg mouse subline, which was obtained by crossing B6;C3-Tg(APP<sup>swe</sup>,PSEN1<sup>dE9</sup>)85Dbo/Mmjax mice (#034829-JAX) with wild-type C57Bl6J/ChG mice. The C57Bl6J/ChG line was obtained from the Charles River UK breeding facility and had been maintained as an isolated colony in pathogen-free conditions of the breeding facility of the Institute of Physiologically Active Compounds for 7 years. The colony was maintained and propagated by crossing transgenic mice with wild-type mice of the same litters.

Experimental and control mice were kept in pathogen-free conditions of the breeding facility of Belgorod State National Research University with an artificial light–dark cycle (12 h light and 12 h dark) at 22–26°C with free access to food and water.

**Genotyping of transgenic mice.** Genomic DNA was isolated from ear biopsy material (approximately 30 mg). A tissue sample was incubated in a lysis solution (100 mM NaCl, 50 mM Tris-HCl, pH 8.0, 2 mM EDTA, 2 mg/mL proteinase K) at 55°C for 12–16 h, and the resulting mixture was heated at 85°C for 40 min.

**Table 1.** Most common transgenic mouse lines that model cerebral amyloidosis

Line (JAX mice)	Mutation	Promoter	Amyloid plaques, age	Reference
PDAPP	hAPP (V717F)	Promoter of platelet-derived growth factor $\beta$ (PDGF- $\beta$ ) gene	6–9 months: cortex, hippocampus, corpus callosum	[14]
APP23 (B6.Cg-Tg(Thy1-APP)3Somm/J)	hAPP <sub>751</sub> (K670N/M671L)	Mouse <i>Thy1</i> promoter	6–8 months: cortex 12–24 months: cortex, hippocampus, thalamus, amygdala	[15]
Tg2576 (B6;SJL-Tg(APP <sup>SWE</sup> )2576Kha)	hAPP <sub>695</sub> (K670N/M671L)	Promoter of hamster prion protein gene	7–8 months: cortex 11–13 months: hippocampus, cerebellum	[16]
Tg-SwDI (C57BL/6-Tg(Thy1-APP <sup>SwDu-tIowa</sup> )BWenv/Mmjax)	hAPP <sub>770</sub> (K670N/M671L) hAPP <sub>770</sub> (E693Q) hAPP <sub>770</sub> (D694N)	Mouse <i>Thy1</i> promoter	3 months: cortex, hippocampus 6 months: olfactory bulbs, thalamus	[17]
3xTg (B6;129-Tg(APP <sup>Swe</sup> ,tauP301L)1Lfa <i>Psen1</i> <sup>tm1Mpm</sup> /Mmjax)	hAPP (K670N/M671L) hMAPT (P301L) mPsen1 (M146V)	Mouse <i>Thy1</i> promoter (APP, MAPT), Mouse <i>Psen1</i> promoter	6 months: cortex, hippocampus 12 months: hippocampus	[18]
APP <sup>swe</sup> /PS1 <sup>dE9</sup> (B6;C3-Tg(APP <sup>swe</sup> ,PSEN1 <sup>dE9</sup> )85Dbo/Mmjax)	Mo/HuAPP (K670N/M671L) hPSEN1 $\Delta$ E9	Promoter of mouse prion protein gene	5–6 months: cortex, hippocampus	[19]
5xFAD (B6SJL-Tg(APP <sup>SwFILon</sup> ,PSEN1* <sup>M146L</sup> *L286V)6799Vas/Mmjax)	hAPP (K670N/M671L) hAPP (V717I) hAPP (I716V) hPSEN1 (M146L) hPSEN1(L286V)	Mouse <i>Thy1</i> promoter	2 months: cortex, subiculum 4 months: spinal cord 6 months: hippocampus, thalamus, olfactory bulbs, basal brain regions	[20]
J20 (B6.Cg-Zbtb <sup>20Tg</sup> (PDGF $\beta$ -APP <sup>SwInd</sup> )20Lms/2Mmjax)	hAPP (K670N/M671L) hAPP (V717F)	Promoter of platelet-derived growth factor $\beta$ (PDGF- $\beta$ ) gene	5–8 months: cortex, hippocampus	[21]
APPPS1 (B6.Cg-Tg(Thy1-APP <sup>Sw</sup> ,Thy1-PSEN1*L166P)21Jckr)	hAPP (K670N/M671L) hPSEN1 (L166P)	Mouse <i>Thy1</i> promoter	6 weeks: cortex 2–3 months: hippocampus 3–5 months: striatum, thalamus	[22]
PS/APP	hAPP (K670N/M671L) hPSEN1 (M146L)	Promoter of hamster prion protein gene Promoter of platelet-derived growth factor $\beta$ (PDGF- $\beta$ ) gene	6 months: cortex, hippocampus 12 months: striatum, thalamus, brainstem	[23], [24], [25]
PS2Tg2576	hAPP (K670N/M671L) hPSEN2 (N141I)	Promoter of hamster prion protein gene Promoter of chicken $\beta$ -actin gene	2–3 months: cortex, hippocampus	[26]

**Table 1.** (Contd.)

Line (JAX mice)	Mutation	Promoter	Amyloid plaques, age	Reference
mThy1-hA $\beta$ PP751	hAPP (K670N/M671L) hAPP (V717I)	Mouse <i>Thy1</i> promoter	3–6 months: cortex 5–7 months: hippocampus, thalamus, olfactory bulbs	[27]
<i>PLB1-triple</i>	hAPP (K670N/M671L) hAPP (V717I) hMAPT (P301L) hMAPT (R406W) hPSEN1 (A246E)	Mouse <i>CaMKII-<math>\alpha</math></i> promoter (APP, MAPT) Promoter of mouse prion protein gene ( <i>PSEN1</i> )	5–6 months: cortex, hippocampus	[28]
<i>knock-in APP</i> (App <sup>NL-G-F</sup> )	Mo/HuAPP (K670N/M671L) Mo/HuAPP (E693G) Mo/HuAPP (I716F)	Mouse <i>APP</i> promoter	2 months: cortex 4 months: hippocampus	[29]
<i>knock-in App</i> <sup>NL-F</sup> Psen1 <sup>P117L/WT</sup>	Mo/HuAPP (K670N/M671L) Mo/HuAPP (I716F) mPsen1 (P117L)	Mouse <i>APP</i> promoter Mouse <i>Psen1</i> promoter	3 months: cortex 12 months: hippocampus	[30]

The lysate was centrifuged at 10000 g for 1 min. The supernatant (1  $\mu$ L) was used as a template in PCR [32].

**Primers.** We used the primers designed by Jankowsky et al. [19] to amplify simultaneously a fragment of the transgenic cassette (if present) and a mouse genomic DNA region. Three primers were added to the reaction mixture: the common reverse primer PrP<sub>rev</sub> (5'-GTG GAT ACC CCC TCC CCC AGC CTA GAC C), which was homologous to a *PrP* sequence contained in the mouse genome and the transgenic cassette; the forward primer PrP<sub>for</sub> (5'-CCT CTT TGT GAC TAT GTG GAC TGA TGT CGG), which was homologous to a sequence present in mouse genomic *PrP* and removed from the MoPrP.Xho vector; and one of the specific forward primers PS1 (5'-CAG GTG GTG GAG CAA GAT G) and APP (5'-CCG AGA TCT CTG AAG TGA AGA TGG ATG), which were homologous to the mutant protein-coding genes contained in the transgenic cassette. The reaction mixture contained 1 $\times$  Taq Turbo buffer (Evrogen, Russia), 0.2 mM each dNTP (Evrogen), 0.5  $\mu$ M each forward primer, 1  $\mu$ M common reverse primer, and 2 units of HS Taq DNA polymerase (Evrogen). Amplification included the initial cycle of 95°C for 3 min; 30 cycles of 95°C for 20 s, 55°C (APP) or 65°C (PS1) for 20 s, and 72°C for 20 s; and the last cycle of 72°C for 2 min.

The amplification products were resolved electrophoretically in 1.5% agarose gel in 1 $\times$  TAE buffer (40 mM Tris-HCl, 20 mM acetic acid, 1 mM EDTA, 0.5  $\mu$ g/mL ethidium bromide) at 120 V for 30 min.

**Histological preparations.** Mice were sacrificed via lethal anesthesia. The brain was dissected and fixed with Carnoy's solution (96% ethanol–chloroform–

glacial acetic acid, 6 : 3 : 1) overnight. Tissue was dehydrated through graded ethanol solutions (75% for h, 96% (I) for 5 min; 96% (II) for 45 min, 100% (I) for 5 min, and 100% (II) for 10 min). The sample was incubated consecutively with 100% ethanol–chloroform (1 : 1) for 30 min, chloroform (I) for 1 h, and chloroform (II) overnight and embedded in paraffin (three times, for 1 h each) at 60°C. A Leica EG1160 tissue embedding station (Leica Biosystems, Germany) was used. Paraffin sections (8  $\mu$ m thick) were mounted on polylysine-coated slides. Then the sections were deparaffinized in a xylene bath for 20 min; rehydrated through graded ethanol solutions (100% for 1 min, 95% for 5 min, and 50% for 5 min); washed three times with deionized water for 5 min; stained with 0.5% Congo Red, 50% ethanol for 5 min; differentiated with 0.2% KOH, 80% ethanol for 1 min; washed three times with deionized water for 5 min; and embedded in the Immu-Mount water-based mounting medium (Thermo Scientific, United States).

## RESULTS AND DISCUSSION

The APP<sup>swe</sup>/PS1<sup>dE9</sup>/Blg mouse subline was obtained by crossing B6;C3-Tg(APP<sup>swe</sup>,PSEN1<sup>dE9</sup>)85Dbo/Mmjax on a mixed C3H/C57Bl6 genetic background with C57Bl6J/ChG mice. To obtain representative groups of test and control age-synchronized mice, related breeders were first obtained in necessary numbers. Mice hemizygous for a transgene cassette were crossed with wild-type mice on the same mixed genetic background, which was formed in previous crosses. Offspring was genotyped by conventional PCR with a pair of specific primers directed to either *PSEN1* or *APP* because the two transgenic cas-

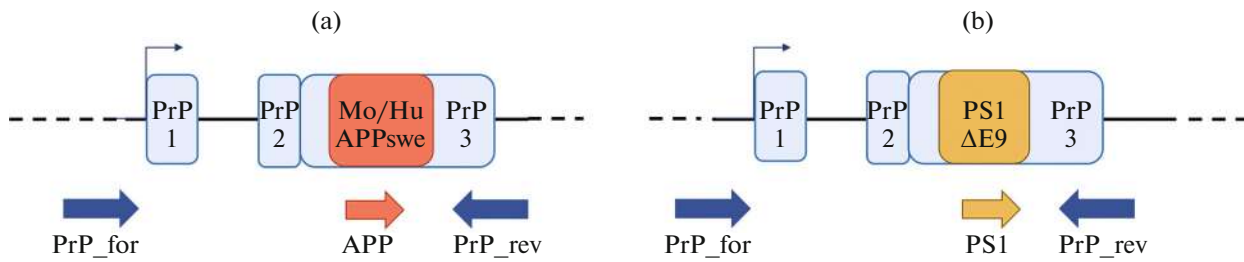


**Fig. 1.** Positions of the primers used to detect the transgene cassettes in the APP<sub>swe</sub>/PS1ΔE9 mouse genome. The cassettes contained (a) the cDNA of the amyloid precursor protein with the Swedish mutation (Mo/Hu APP<sub>swe</sub>) and (b) the cDNA of the human presenilin 1 gene with a deletion of exon 9 (PS1ΔE9). The two cassettes are integrated in the same locus in chromosome 9 and are each expressed under the control of a separate mouse prion protein gene (*PrP*) promoter. The forward primer PrP\_for is homologous to a region of the endogenous mouse *PrP* gene. The reverse primer PrP\_rev is homologous to a sequence contained in both endogenous *PrP* and the *PrP* sequence contained in the transgene cassettes. The forward primers APP and PS1 specifically recognize their target sequences within the respective transgene cassettes. Designations: PrP1, exon 1; PrP2, exon 2; PrP3, exon 3. The forward and reverse primers are shown with arrows.

settes were in the same locus of chromosome 9 in the mouse genome. The positions of primers used to amplify the transgenic cassettes are schematically shown in Fig. 1. Example genotyping results are shown in Fig. 2 for each transgene cassette.

Integration of the two transgene cassettes in the same locus of the mouse genome [19] made it possible to perform genotyping by detecting only one of the cassettes. Genotyping results confirmed that the two transgene cassettes were preserved through several mouse generations. Thus, primers to one of the transgenes are possible to use in PCR for genotyping APP<sub>swe</sub>/PS1ΔE9/Blg mice. We recommend that the presence of both of the transgene cassettes in the mouse genome be verified in every third or fourth generation after the formation of test and control samples.

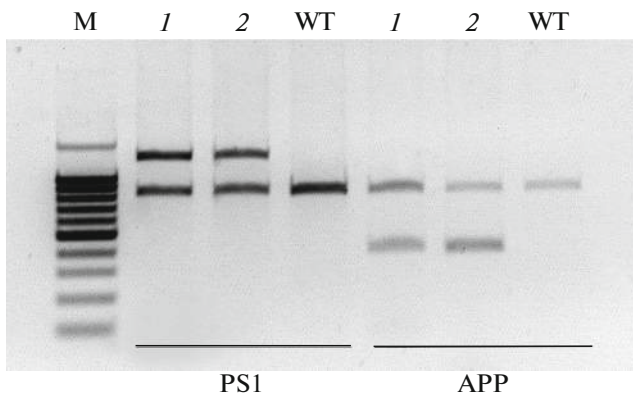


**Fig. 2.** Detection of the transgene cassettes in the genomes of APP<sub>swe</sub>/PS1ΔE9/Blg mice by PCR. A mouse prion protein gene fragment (750 bp) was amplified in all samples (endogenous control). Amplification of the 750-bp fragment only is characteristic of wild-type mice (WT). Transgenic APP<sub>swe</sub>/PS1ΔE9/Blg mice (lanes 1 and 2) display an additional 1.3-kb fragment, which is amplified from the mutant *PSEN1* gene, or an additional 400-bp fragment, which is amplified from the mutant *APP* gene. M, 100+ bp marker (Evrogen).

To form the test groups, APP<sub>swe</sub>/PS1ΔE9/Blg mice were crossed with wild-type mice from previous litters. A considerable difference in survival was not observed between transgenic mice and wild-type mice from the same litters. Genotyping performed in 315 mice showed that 52.4% of mice carried the transgene cassette, while 47.6% of the mice lacked genome modification.

Breeder pairs included transgenic females and wild-type males or transgenic males and wild-type females. The breeders were used at 2–4 months of age. A fertility testing in APP<sub>swe</sub>/PS1ΔE9/Blg females showed that 74% of transgenic females and 84% of wild-type females were fertile. Based on the total number of offspring, the number of offspring per female was calculated and found to be much the same in APP<sub>swe</sub>/PS1ΔE9/Blg and wild-type females (Table 2).

Thus, we showed that APP<sub>swe</sub>/PS1ΔE9/Blg do not significantly differ in survival and fertility from control wild-type mice. The results allowed us to plan the formation of breeder pairs to obtain experimental groups and to achieve the required numbers of transgenic mice in the experimental cohorts.

A cross-β structure of the protein involved is a feature of amyloid-type inclusions and determines their binding with specific dyes, such as Congo Red and Thioflavin S [2]. The age at which histological signs of cerebral amyloidosis become detectable in the brain of APP<sub>swe</sub>/PS1ΔE9 mice and the progression dynamics of the neurodegenerative processes slightly differ between different laboratories. The pathology is most often detected in 6-month-old mice and is broadly spread through the hippocampus and cerebral cortex at this age [33]. Data on the progression of amyloidosis vary depending on the method employed in the analysis, the size of amyloid inclusions (whether medium-sized and small inclusions are scored together with large inclusions), the use of the Ambercrombie correction for the possibility of scoring the same inclusion in several serial sections, the tissue staining method (staining with special dyes, such as

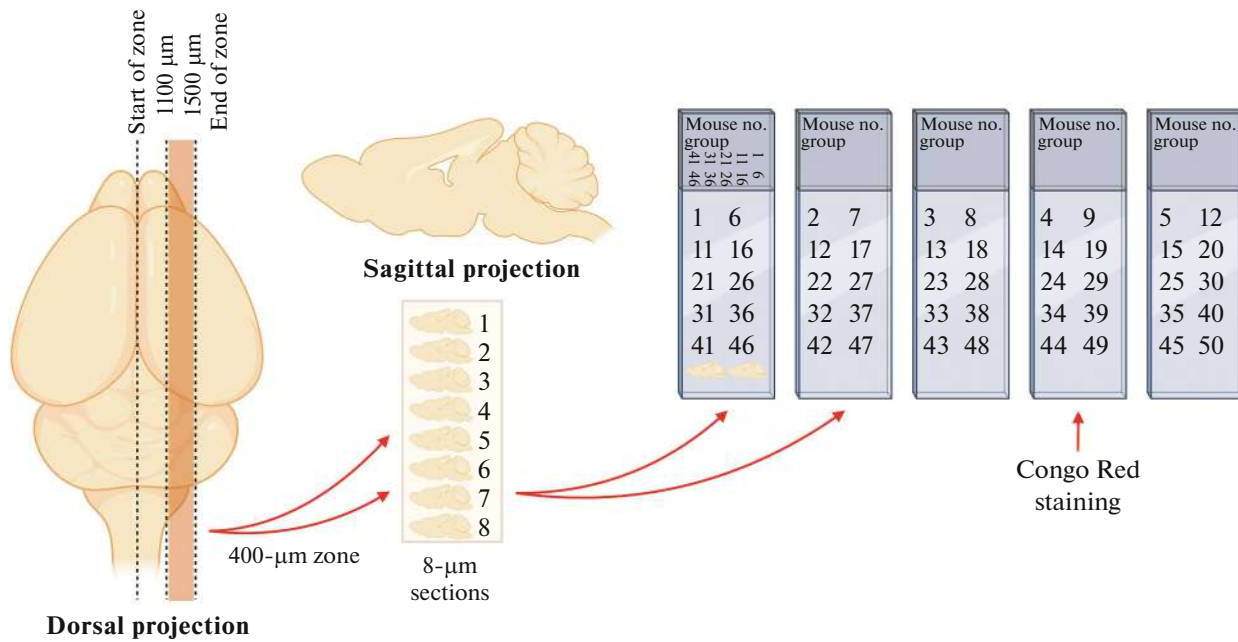


**Fig. 3.** Arrangement of brain sections in histological preparations. Sections were obtained from a 400- $\mu$ m-thick zone of the brain and arranged on five slides at 10 sections per slide. Every fifth section was placed on the same slide.

Congo Red and Thioflavin S, or antibodies against A $\beta$ ), and the detection method (detection within a certain wavelength range or with additional use of polarized light) [4, 34, 35]. A detail characteristic of the subline under study is of immense importance for its use as a model of cerebral amyloidosis.

The brains of APP<sup>swe</sup>/PS1<sup>dE9</sup>/Btg mice were examined histologically at ages of 5.5 and 10 months. To perform a morphometric analysis of inclusions, section groups were formed as shown in Fig. 3.

To estimate the amount of amyloid inclusions in the hippocampus and cerebral cortex, sections of a cerebral hemisphere were obtained from APP<sup>swe</sup>/PS1<sup>dE9</sup>/Btg mice and stained with Congo Red (Fig. 4). Large amyloid inclusions, along with small and medium-sized ones, were detected in the cortex and hippocampus as

early as 5.5 months of age in transgenic mice. The number and size of aggregates in the brain increased by 10 months of age in transgenic mice. Amyloid inclusions were not detected in the brains of control wild-type mice. According to published data, 24-month-old mice were the oldest APP<sup>swe</sup>/PS1<sup>dE9</sup> mice used to study the formation of amyloid inclusions [33].

The rates of the formation of pathological A $\beta$  aggregates in the cortex and hippocampus were estimated in transgenic APP/PS1 and control mice at 5.5 and 10 months of age (Table 3).

Human AD may develop over several decades before the earliest signs become detectable. The progression of A $\beta$  aggregation in the hippocampus and cortex was assessed by comparing young transgenic mice (5.5 months of age) with aging mice (10 months

**Table 2.** Female fertility in reproduction of transgenic mice

Breeder females	Total females let to mate	Females not getting pregnant	Total offspring	Mean number of offspring per litter
APP <sup>swe</sup> /PS1 <sup>dE9</sup> /Btg	35	9	140	5.38
Wild type	38	6	175	5.47

**Table 3.** Morphometric analysis of inclusions in transgenic APP<sup>swe</sup>/PS1<sup>dE9</sup>/Btg mice at 5.5 and 10 months of age

Age, months	Hippocampal aggregates	Cortical aggregates
5.5	5.010 $\pm$ 0.886	30.11 $\pm$ 4.714
10	24.37 $\pm$ 2.929	125.1 $\pm$ 13.50

Results were averaged over 10 mice.

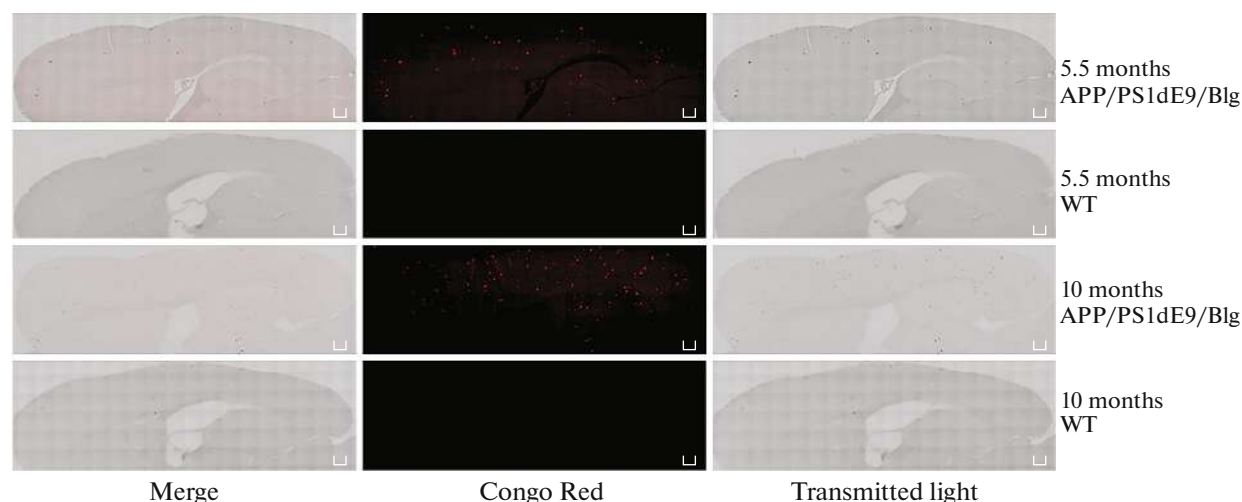


**Fig. 4.** Histological analysis of A $\beta$  inclusions in brain sections of transgenic APP<sup>swE</sup>/PS1dE9/Blg and control wild-type mice at 5.5 and 10 months of age. Staining with Congo Red. Bar, 200  $\mu$ m.

of age). The numbers of inclusions in the hippocampus and cortex increased in the aging mice by a factors of almost 5 and 4, respectively ( $p < 0.0001$ , Student's  $t$ -test).

Our findings agree with the published results of counting amyloid plaques in the brain in transgenic APP<sup>swE</sup>/PS1dE9 males. On average, approximately 20 plaques were detected in the cortex and approximately 5, in the hippocampus at an age of 4 months, while an approximately four times greater number of inclusions in the cortex and a twice greater number of inclusions in the hippocampus were observed in 10-month-old mice [4].

Injections of the synthetic tetrapeptides HAEE and RADD have shown efficacy as therapeutic means to reduce the level of the aggregated A $\beta$  form in vivo. The tetrapeptides specifically bind to the EVHH site of the A $\beta$  peptide and thus suppress its Zn-mediated dimerization, decreasing the level of amyloid plaques detectable in the cortex and hippocampus of transgenic APP<sup>swE</sup>/PS1dE9 mice at 7 months of age [36]. It has also been demonstrated experimentally that Asp isomerization and Ser8 phosphorylation in the A $\beta$ 42 peptide may prevent its Zn-dependent aggregation. Injections of the synthetic peptide isoD7-pS8-A $\beta$ 42 with these modifications ensured a significant (more than threefold) reduction in the number of amyloid inclusions in the brain of 8-month-old APP<sup>swE</sup>/PS1dE9 mice ( $7.4 \pm 2.8$ ) as compared with untreated transgenic mice ( $28.7 \pm 4.6$ ) [37]. Injections of the synthetic peptide pS8-A $\beta$ 42 with phosphorylated Ser8 similarly caused a 1.5-fold decrease in the number of amyloid-type aggregates in the hippocampus of 8-month-old transgenic APP<sup>swE</sup>/PS1dE9 mice ( $18.3 \pm 0.94$ ) as compared with untreated control mice ( $28.7 \pm 4.6$ ) [38].

Thus, the number of A $\beta$  aggregates in the brain is an important parameter in APP<sup>swE</sup>/PS1dE9 mice and

should be considered when designing therapeutic strategies to slow down the AD progression.

#### FUNDING

This work was supported by the Ministry of Science and Higher Education of the Russian Federation (agreement no. 075-15-2021-1346). Animal procedures were funded by the State Task of the Laboratory of Genetic Technologies and Genome Editing for Biomedicine and Animal Health—FWZG-2021-0016

#### COMPLIANCE WITH ETHICAL STANDARDS

*Conflict of interests.* The authors declare that they have no conflict of interest.

*Statement of the welfare of animals.* Experiments with animals obeyed the “Rules of Laboratory Practice in the Russian Federation” (no. 199n dated April 1, 2016). The study was approved by the Ethics Committee at the Belgorod State University (Minutes no. 02.21-4 dated February 8, 2021).

#### REFERENCES

1. Konttinen H., Cabral-da-Silva M.E.C., Ohtonen S., Wojciechowski S., Shakirzyanova A., Caligola S., Gigugno R., Ishchenko Y., Hernandez D., Fazaludeen M.F., Eamen S., Budia M.G., Fagerlund I., Scoyni F., Korhonen P., Huber N., Haapasalo A., Hewitt A.W., Vickers J., Smith G.C., Oksanen M., Graff C., Kanninen K.M., Lehtonen S., Propson N., Schwartz M.P., Pebay A., Koistinaho J., Ooi L., Malm T. 2019. PSEN1DeltaE9, APP<sup>swE</sup>, and APOE4 confer disparate phenotypes in human iPSC-derived microglia. *Stem. Cell Rep.* **13**, 669–683.
2. Shelkovnikova T.A., Kulikova A.A., Tsvetkov F.O., Peters O., Bachurin S.O., Bukhman V.L., Ninkina N.N. 2012. Proteinopathies, neurodegenerative disorders

- with protein aggregation-based pathology. *Mol. Biol. (Moscow)*. **46**, 362–374.
3. Masters C.L., Bateman R., Blennow K., Rowe C.C., Sperling R.A., Cummings J.L. 2015. Alzheimer's disease. *Nat. Rev. Dis. Primers*. **1**, 15056.
  4. Kozin S.A., Cheglakov I.B., Ovsepyan A.A., Telegin G.B., Tsvetkov P.O., Lisitsa A.V., Makarov A.A. 2013. Peripherally applied synthetic peptide isoAsp7-Abeta(1-42) triggers cerebral beta-amyloidosis. *Neurotoxicity Res*. **24**, 370–376.
  5. Evin G., Li Q.X. 2012. Platelets and Alzheimer's disease: potential of APP as a biomarker. *W. J. Psychiatry*. **2**, 102–113.
  6. Vetrivel K.S., Thinakaran G. 2006. Amyloidogenic processing of beta-amyloid precursor protein in intracellular compartments. *Neurology*. **66**, S69–73.
  7. De Strooper B., Annaert W. 2010. Novel research horizons for presenilins and gamma-secretases in cell biology and disease. *Annu. Rev. Cell. Dev. Biol*. **26**, 235–260.
  8. Manczak M., Kandimalla R., Yin X., Reddy P.H. 2018. Hippocampal mutant APP and amyloid beta-induced cognitive decline, dendritic spine loss, defective autophagy, mitophagy and mitochondrial abnormalities in a mouse model of Alzheimer's disease. *Hum. Mol. Genet*. **27**, 1332–1342.
  9. Pan J.X., Sun D., Lee D., Xiong L., Ren X., Guo H.H., Yao L.L., Lu Y., Jung C., Xiong W.C. 2021. Osteoblastic Swedish mutant APP expedites brain deficits by inducing endoplasmic reticulum stress-driven senescence. *Commun. Biol*. **4**, 1326.
  10. Tatarnikova O.G., Orlov M.A., Bobkova N.V. 2015. Beta-amyloid and tau protein: structure, interaction and prion-like properties. *Usp. Biol. Khim*. **55**, 351–390.
  11. Armstrong R.A. 2019. Risk factors for Alzheimer's disease. *Folia Neuropathol*. **57**, 87–105.
  12. Jankowsky J.L., Fadale D.J., Anderson J., Xu G.M., Gonzales V., Jenkins N.A., Copeland N.G., Lee M.K., Younkin L.H., Wagner S.L., Younkin S.G., Borchelt D.R. 2004. Mutant presenilins specifically elevate the levels of the 42 residue beta-amyloid peptide in vivo: evidence for augmentation of a 42-specific gamma secretase. *Hum. Mol. Genet*. **13**, 159–170.
  13. Sasaguri H., Hashimoto S., Watamura N., Sato K., Takamura R., Nagata K., Tsubuki S., Ohshima T., Yoshiki A., Sato K., Kumita W., Sasaki E., Kitazume S., Nilsson P., Winblad B., Saito T., Iwata N., Saido T.C. 2022. Recent advances in the modeling of Alzheimer's disease. *Front. Neurosci*. **16**, 807473.
  14. Games D., Adams D., Alessandrini R., Barbour R., Borthellette P., Blackwell C., Carr T., Clemens J., Donaldson T., Gillespie F., Guido T., Hagopian S., Johnson-Wood K., Khan K., Lee M., Leibowitz P., Lieberburg I., Little S., Masliah E., McConlogue L., Montoya-Zavala M., Mucke L., Paganini L., Penniman E., Power M., Schenk D., Seubert P., Snyder B., Soriano F., Tan H., Vitale J., Wadsworth S., Wolozin B., Zhao J. 1995. Alzheimer-type neuropathology in transgenic mice overexpressing V717F beta-amyloid precursor protein. *Nature*. **373**, 523–527.
  15. Kuo Y.M., Beach T.G., Sue L.I., Scott S., Layne K.J., Kokjohn T.A., Kalback W.M., Luehrs D.C., Vishnivetskaya T.A., Abramowski D., Sturchler-Pierrat C., Staufenbiel M., Weller R.O., Roher A.E. 2001. The evolution of A beta peptide burden in the APP23 transgenic mice: implications for A beta deposition in Alzheimer disease. *Mol. Med*. **7**, 609–618.
  16. Hsiao K., Chapman P., Nilsen S., Eckman C., Harigaya Y., Younkin S., Yang F., Cole G. 1996. Correlative memory deficits, Abeta elevation, and amyloid plaques in transgenic mice. *Science*. **274**, 99–102.
  17. Davis J., Xu F., Deane R., Romanov G., Previti M.L., Zeigler K., Zlokovic B.V., Van Nostrand W.E. 2004. Early-onset and robust cerebral microvascular accumulation of amyloid beta-protein in transgenic mice expressing low levels of a vasculotropic Dutch/Iowa mutant form of amyloid beta-protein precursor. *J. Biol. Chem*. **279**, 20296–20306.
  18. Oddo S., Caccamo A., Shepherd J.D., Murphy M.P., Golde T.E., Kaye R., Metherate R., Mattson M.P., Akbari Y., LaFerla F.M. 2003. Triple-transgenic model of Alzheimer's disease with plaques and tangles: intracellular Abeta and synaptic dysfunction. *Neuron*. **39**, 409–421.
  19. Jankowsky J.L., Slunt H.H., Ratovitski T., Jenkins N.A., Copeland N.G., Borchelt D.R. 2001. Co-expression of multiple transgenes in mouse CNS: a comparison of strategies. *Biomol. Engin*. **17**, 157–165.
  20. Oakley H., Cole S.L., Logan S., Maus E., Shao P., Craft J., Guillozet-Bongaarts A., Ohno M., Disterhoft J., Van Eldik L., Berry R., Vassar R. 2006. Intraneuronal beta-amyloid aggregates, neurodegeneration, and neuron loss in transgenic mice with five familial Alzheimer's disease mutations: potential factors in amyloid plaque formation. *J. Neurosci*. **26**, 10129–10140.
  21. Mucke L., Masliah E., Yu G.Q., Mallory M., Rockenstein E.M., Tatsuno G., Hu K., Kholodenko D., Johnson-Wood K., McConlogue L. 2000. High-level neuronal expression of abeta 1–42 in wild-type human amyloid protein precursor transgenic mice: synaptotoxicity without plaque formation. *J. Neurosci*. **20**, 4050–4058.
  22. Radde R., Bolmont T., Kaeser S.A., Coomaraswamy J., Lindau D., Stoltze L., Calhoun M.E., Jaggi F., Wolburg H., Gengler S., Haass C., Ghetti B., Czech C., Holscher C., Mathews P.M., Jucker M. 2006. Abeta42-driven cerebral amyloidosis in transgenic mice reveals early and robust pathology. *EMBO Rep*. **7**, 940–946.
  23. Holcomb L., Gordon M.N., McGowan E., Yu X., Benkovic S., Jantzen P., Wright K., Saad I., Mueller R., Morgan D., Sanders S., Zehr C., O'Campo K., Hardy J., Prada C.M., Eckman C., Younkin S., Hsiao K., Duff K. 1998. Accelerated Alzheimer-type phenotype in transgenic mice carrying both mutant amyloid precursor protein and presenilin 1 transgenes. *Nat. Med*. **4**, 97–100.
  24. Kurt M.A., Davies D.C., Kidd M., Duff K., Rolph S.C., Jennings K.H., Howlett D.R. 2001. Neurodegenerative changes associated with beta-amyloid deposition in the brains of mice carrying mutant amyloid precursor protein and mutant presenilin-1 transgenes. *Exp. Neurol*. **171**, 59–71.



25. McGowan E., Sanders S., Iwatsubo T., Takeuchi A., Saido T., Zehr C., Yu X., Uljon S., Wang R., Mann D., Dickson D., Duff K. 1999. Amyloid phenotype characterization of transgenic mice overexpressing both mutant amyloid precursor protein and mutant presenilin 1 transgenes. *Neurobiol. Dis.* **6**, 231–244.
26. Toda T., Noda Y., Ito G., Maeda M., Shimizu T. 2011. Presenilin-2 mutation causes early amyloid accumulation and memory impairment in a transgenic mouse model of Alzheimer's disease. *J. Biomed. Biotechnol.* **2011**, 617974.
27. Rockenstein E., Mallory M., Mante M., Sisk A., Masliha E. 2001. Early formation of mature amyloid-beta protein deposits in a mutant APP transgenic model depends on levels of Abeta(1-42). *J. Neurosci. Res.* **66**, 573–582.
28. Platt B., Drever B., Koss D., Stoppelkamp S., Jyoti A., Plano A., Utan A., Merrick G., Ryan D., Melis V., Wan H., Mingarelli M., Porcu E., Scrocchi L., Welch A., Riedel G. 2011. Abnormal cognition, sleep, EEG and brain metabolism in a novel knock-in Alzheimer mouse, PLB1. *PLoS One.* **6**, e27068.
29. Saito T., Matsuba Y., Mihira N., Takano J., Nilsson P., Itohara S., Iwata N., Saido T.C. 2014. Single App knock-in mouse models of Alzheimer's disease. *Nat. Neurosci.* **17**, 661–663.
30. Sato K., Watamura N., Fujioka R., Mihira N., Sekiguchi M., Nagata K., Ohshima T., Saito T., Saido T.C., Sasaguri H. 2021. A third-generation mouse model of Alzheimer's disease shows early and increased cored plaque pathology composed of wild-type human amyloid beta peptide. *J. Biol. Chem.* **297**, 101004.
31. Jankowsky J.L., Xu G., Fromholt D., Gonzales V., Borchelt D.R. 2003. Environmental enrichment exacerbates amyloid plaque formation in a transgenic mouse model of Alzheimer disease. *J. Neuropathol. Exp. Neurol.* **62**, 1220–1227.
32. Lysikova E.A., Kukharsky M.S., Chaprov K.D., Vasilieva N.A., Roman A.Y., Ovchinnikov R.K., Deykin A.V., Ninkina N., Buchman V.L. 2019. Behavioural impairments in mice of a novel FUS transgenic line recapitulate features of frontotemporal lobar degeneration. *Genes Brain Behav.* **18**, e12607.
33. D'Angelo C., Costantini E., Salvador N., Marchioni M., Di Nicola M., Greig N.H., Reale M. 2021. nAChRs gene expression and neuroinflammation in APP<sup>swe</sup>/PS1<sup>dE9</sup> transgenic mouse. *Sci. Rep.* **11**, 9711.
34. Kuhla A., Ruhlmann C., Lindner T., Polei S., Hadlich S., Krause B.J., Vollmar B., Teipel S.J. 2017. APP<sup>swe</sup>/PS1<sup>dE9</sup> mice with cortical amyloid pathology show a reduced NAA/Cr ratio without apparent brain atrophy: a MRS and MRI study. *Neuroimage Clin.* **15**, 581–586.
35. Pezzini A., Del Zotto E., Volonghi I., Giossi A., Costa P., Padovani A. 2009. Cerebral amyloid angiopathy: a common cause of cerebral hemorrhage. *Curr. Med. Chem.* **16**, 2498–2513.
36. Tsvetkov P.O., Cheglakov I.B., Ovsepyan A.A., Mediannikov O.Y., Morozov A.O., Telegin G.B., Kozin S.A. 2015. Peripherally applied synthetic tetrapeptides HAEE and RADD slow down the development of cerebral beta-amyloidosis in AbetaPP/PS1 transgenic mice. *J. Alzheimer's Dis.* **46**, 849–853.
37. Kozin S.A., Barykin E.P., Telegin G.B., Chernov A.S., Adzhubei A.A., Radko S.P., Mitkevich V.A., Makarov A.A. 2018. Intravenously injected amyloid-beta peptide with isomerized Asp7 and phosphorylated Ser8 residues inhibits cerebral beta-amyloidosis in AbetaPP/PS1 transgenic mice model of Alzheimer's disease. *Front. Neurosci.* **12**, 518.
38. Barykin E.P., Petrushanko I.Y., Kozin S.A., Telegin G.B., Chernov A.S., Lopina O.D., Radko S.P., Mitkevich V.A., Makarov A.A. 2018. Phosphorylation of the amyloid-beta peptide inhibits zinc-dependent aggregation, prevents Na,K-ATPase inhibition, and reduces cerebral plaque deposition. *Front. Mol. Neurosci.* **11**, 302.

*Translated by T. Tkacheva*